

CHUNK-WISE ATTENTION TRANSDUCERS FOR FAST AND ACCURATE STREAMING SPEECH-TO-TEXT

Hainan Xu, Vladimir Bataev, Travis M. Bartley, Jagadeesh Balam

NVIDIA Corporation.
hainanx@nvidia.com

ABSTRACT

We propose Chunk-wise Attention Transducer (CHAT), a novel extension to RNN-T models that processes audio in fixed-size chunks while employing cross-attention within each chunk. This hybrid approach maintains RNN-T’s streaming capability while introducing controlled flexibility for local alignment modeling. CHAT significantly reduces the temporal dimension that RNN-T must handle, yielding substantial efficiency improvements: up to 46.2% reduction in peak training memory, up to 1.36X faster training, and up to 1.69X faster inference. Alongside these efficiency gains, CHAT achieves consistent accuracy improvements over RNN-T across multiple languages and tasks – up to 6.3% relative WER reduction for speech recognition and up to 18.0% BLEU improvement for speech translation. The method proves particularly effective for speech translation, where RNN-T’s strict monotonic alignment hurts performance. Our results demonstrate that the CHAT model offers a practical solution for deploying more capable streaming speech models without sacrificing real-time constraints.

Index Terms— streaming model, speech recognition, speech translation, RNN-T, attention model

1. INTRODUCTION

Streaming speech processing systems [1] require models that can process audio incrementally while maintaining high accuracy and low latency. RNN-T [2] is a popular model for such processing, due to its frame-synchronous nature. However, RNN-T models are monotonic in nature, limiting its modeling capacity for more complex tasks that require flexible alignments. Further, RNN-T training is computationally costly, requiring substantial time and memory during training due to the forward-backward algorithm over the alignment lattice.

Numerous works have proposed ways to improve the modeling capacity and/or efficiency of RNN-T models. Multi-blank Transducers [3], Token-and-Duration Transducers (TDT) [4], and their variants [5] propose explicitly modeling frame duration alignment of individual text tokens, bringing inference speedup and slight accuracy gains. In terms of architecture improvements, more sophisticated

models [6], [7] are shown to outperform LSTM encoders. Stateless predictors [8] achieve similar accuracy as LSTM variants, with improved efficiency. Meanwhile, [9] proposed a joiner with attention-pooling operation to improve performance for speech translation. [10], [11], [12] improved the speed of RNN-T inference.

In this work, we enhance the RNN-T architecture to operate on chunks of input frames while enabling the joint network to perform cross-attention within chunks. This approach, which we term *Chunk-wise Attention Transducer* (CHAT), maintains RNN-T’s streaming capability and computational advantages while introducing controlled flexibility in local alignment modeling. This work shares similarity with [13], with the added benefit that no time-stamp information is needed for training our model. Some of the most notable improvements we see with the CHAT model over RNN-T are,

category	CHAT over RNN-T
peak training GPU memory	46.2% reduction
training speed	1.36X faster
inference speed	1.69X faster
ASR WER	6.3% reduction
AST BLEU	18.0% increase

2. BACKGROUND

2.1. RNN-Transducer

An RNN-T consists of an encoder, a predictor, and a joiner. The encoder processes acoustic input $\mathbf{x} = (x_1, \dots, x_T)$ to produce encoded representations $\mathbf{h}^{\text{enc}} = (h_1^{\text{enc}}, \dots, h_T^{\text{enc}})$ ¹. The predictor takes history text $\mathbf{y}_{\leq u} = (y_1, y_2, \dots, y_u)$ to generate predictor states h^{pred} . The joiner combines these representations and computes the probability distribution over the vocabulary plus a blank symbol:

$$P(z_{t,u+1} | h_t, \mathbf{y}_{\leq u}) = \text{Softmax}(\text{Joiner}(h_t^{\text{enc}}, h_u^{\text{pred}})) \quad (1)$$

An RNN-T model can be trained without token level time-stamps, achieved by summing over all possible alignments

¹The encoder can also perform up/down-sampling so the output length can be different than the input. We omit this in our notations for simplicity.

corresponding to the text output, using a forward-backward algorithm on a $T \times U$ lattice. During inference, RNN-T operates in a frame-synchronous manner. At each frame of h_t^{enc} , and based on the current text history h_t^{pred} , the model decides whether to emit a non-blank symbol (advancing the label pointer) or a blank symbol (advancing the time pointer).

2.2. Chunk-based Streaming Encoder

While RNN-T models support streaming processing over the encoder outputs \mathbf{h}^{enc} , the computation of \mathbf{h}^{enc} doesn't naturally support streaming w.r.t acoustic inputs (x_1, \dots, x_T) . A standard approach to ensure the encoder's streaming compatibility is to enforce causal dependencies such that: for all t , h_t^{enc} exclusively depends on past and current inputs $\mathbf{x}_{\leq t}$.

However, this constraint is suboptimal in practical deployment scenarios. Real-world streaming systems typically operate on audio chunks rather than individual frames, as frame-by-frame processing incurs prohibitive computational overhead due to frequent attention weight recomputation. A better alternative is a cache-aware chunk-based streaming encoder described in [14], where the input sequence is partitioned into non-overlapping temporal chunks $\mathbf{X} = \{\mathbf{X}_1, \mathbf{X}_2, \dots, \mathbf{X}_C\}$. In such chunk-aware processing, frames within a chunk have access to all other frames in the same chunk as well as a limited number of previous chunks, enabling bidirectional attention within chunk boundaries while maintaining streaming capability through activation caching mechanisms. This formulation preserves essential streaming properties by maintaining independence from future chunks $\mathbf{X}_{j>c}$ while enabling full utilization of intra-chunk contextual information.

2.3. RNN-T Joiner

The RNN-T joiner combines representations from the encoder and predictor, serving as the component that integrates acoustic information from the encoder with linguistic context from the predictor to produce output token probabilities. Given an encoder output $\mathbf{h}_t^{\text{enc}} \in \mathbb{R}^{d_{\text{enc}}}$ at time step t and a predictor output $\mathbf{h}_u^{\text{pred}} \in \mathbb{R}^{d_{\text{pred}}}$ at label step u , the standard RNN-T joiner performs a simple additive combination followed by a nonlinear transformation (typically ReLU), before projecting to the vocabulary space. Formally,

$$h_{t,u}^{\text{joint}} = \text{ReLU}(W_{\text{enc}}h_t^{\text{enc}} + W_{\text{pred}}h_u^{\text{pred}}) \quad (2)$$

$$p_{t,u} = \text{softmax}(W_{\text{out}}h_{t,u}^{\text{joint}}) \quad (3)$$

where $W_{\text{enc}} \in \mathbb{R}^{d_{\text{joint}} \times d_{\text{enc}}}$ and $W_{\text{pred}} \in \mathbb{R}^{d_{\text{joint}} \times d_{\text{pred}}}$ are learned projection matrices that map the encoder and predictor representations to a common joint space of dimension d_{joint} . $W_{\text{out}} \in \mathbb{R}^{(|\mathcal{V}|+1) \times d_{\text{joint}}}$ projects the joint representation to the vocabulary space.²

²Actually those are all implemented with `torch.nn.Linear()` and we omit the bias terms in the Equations for brevity.

3. METHOD

3.1. The Big Picture

CHAT models maintain most of the RNN-T architecture, with identical predictor and encoder and loss/gradient computation in training, but with a very different joiner architecture. We also change the interface between the encoder and joiner: instead of single frames, the encoder passes chunks of frames into the joiner. The procedure regarding model prediction is also the same as RNN-T,

- if blank is emitted, then we move on to the next chunk,
- otherwise, we stay at the same chunk, update the predictor representation with the newly predicted token.

CHAT models emit much fewer blank emissions compared to RNN-T. Note with RNN-T, the number of blank tokens always equals the sequence length T , and CHAT reduces blank emissions by the factor of the chunk-size.

3.2. Attention Joiner Architecture

Our improved joiner works as follows: given a chunk of encoder output representations $h_t^{\text{enc}} \in \mathbb{R}^{d_{\text{enc}}}$ for consecutive time steps t within a chunk, and a predictor output $h^{\text{pred}} \in \mathbb{R}^{d_{\text{pred}}}$, the joiner employs a multi-head attention mechanism to selectively aggregate encoder information. For simplicity, we describe the single-head attention procedure here.

Let the chunk-size be C , such that for the n -th chunk, the time indices are $t \in \{Cn, Cn+1, \dots, Cn+C-1\}$. First, we append an all-zero frame to the end of chunk, increases the actual chunk dimension from C to $C+1$. This added frame is treated equally as other frames during the subsequent attention operation, and is so that the model has something to attend to in order to emit the "blank" token.

The joiner utilizes three learned projection matrices: $W_Q \in \mathbb{R}^{d_{\text{pred}} \times d_{\text{joint}}}$, $W_K \in \mathbb{R}^{d_{\text{enc}} \times d_{\text{joint}}}$, and $W_V \in \mathbb{R}^{d_{\text{enc}} \times d_{\text{joint}}}$. The attention computation proceeds as follows:

$$q_u = W_Q h_u^{\text{pred}} \quad (4)$$

$$k_t = W_K h_t^{\text{enc}} \quad \forall t \text{ in chunk}(n) \quad (5)$$

$$v_t = W_V h_t^{\text{enc}} \quad \forall t \text{ in chunk}(n) \quad (6)$$

Note, $\text{chunk}(n)$ includes the added zero frame. Then we compute attention weights via scaled dot-product:

$$\alpha_{t,u} = \frac{\exp\left(\frac{q_u^T k_t}{\sqrt{d_{\text{joint}}}}\right)}{\sum_{j \text{ in chunk}(n)} \exp\left(\frac{q_u^T k_j}{\sqrt{d_{\text{joint}}}}\right)} \quad (7)$$

The attended encoder representation is then obtained as:

$$c_{n,u} = \sum_{t \text{ in chunk}(n)} \alpha_{t,u} v_t \quad (8)$$

Similar to Equation 2, we add predictor representations and perform non-linearity:

$$h_{n,u}^{\text{joint}} = \text{ReLU}(c_{n,u} + h_u^{\text{pred}}) \quad (9)$$

Finally, the joint representation is projected to the vocabulary space and normalized to produce token probabilities:

$$p_{n,u} = \text{softmax}(W_{\text{out}} h_{n,u}^{\text{joint}}) \quad (10)$$

4. EXPERIMENTS

We conduct experiments using the NeMo [15] toolkit, comparing CHAT models with RNN-T. Both of them use FastConformer [16] encoder, and LSTM predictor. We use NeMo’s recommended configuration of FastConformerLarge, with around 110M parameters. The encoder has 17 layers of conformer block, with model dimension 512, and convolution kernel-size 9. Three consecutive 2X convolution-based subsampling operations are performed at the beginning of the encoder, and both the subsampling and convolution in conformer blocks are causal in nature. The chunk size is set to 12 frames, equivalent to 960ms of audio with 10ms speech frames and 8X subsampling resulted from the encoder. In terms of the attention, a frame in a chunk can attend to any frame in the same chunk, as well as from the previous 6 chunks. The attention in the joiner uses num-head=4.³

We evaluate CHAT on speech-to-text recognition and translation tasks, using metrics word-error-rate (WER) and BLEU score, respectively. For all evaluation runs, we run checkpoint averaging on the best-performing checkpoints achieved from up to 500k update steps.

4.1. Speech Recognition Performance

Table 1 shows the ASR performance (WER%) and inference speed (total number of seconds to decode the dataset) across different datasets. For English, we train and evaluate on the Librispeech dataset. For German, we train on the

³The rest of the configuration can be found by searching `fastconformer_transducer_bpe_streaming.yaml` from the NeMo repository.

Table 1: English and German ASR accuracy and inference speed (WER% / decoding time (seconds, with batch=1))

Model	English		German	
	testclean	testother	vox	mls
RNNT	3.01 / 157	7.61 / 149	11.56 / 140	7.23 / 390
CHAT	2.82 / 93	7.45 / 90	11.51 / 86	7.01 / 238
rel. wer diff	-6.3%	-2.1%	-0.43%	-3.0%
rel. speed up	1.69X	1.66X	1.63X	1.64X

Table 2: Speech Translation Results (BLEU)

Model	EN-DE	EN-ZH	EN-CA
RNN-T	29.44	34.01	18.95
CHAT	32.33	39.55	23.1
rel. diff	+9.8%	+16.3%	+18.0%

Common Voice [17], Voxpopuli (vox) [18], and Multilingual Librispeech (mls) [19] datasets, and evaluate on the test sets of vox and mls. We see that CHAT achieves consistent improvements (up to 6.3% relative) over RNN-T baselines; efficiency-wise, CHAT runs significantly faster, with up to 1.69X speedup (batch=1) compared to RNN-T baselines.

4.2. Speech Translation Performance

Table 2 presents speech translation results on English (EN) to German (DE), Chinese (ZH) and Catalan (CA). For DE and ZH translation, we train on a collection of public datasets as described in [20]. For Catalan, we exclusively train on the relative subset of the Covost corpus [21]. We evaluate all models on the respective Covost test datasets. CHAT shows substantial improvements over RNN-T measured by BLEU score, as much as 18.0% relative gain, demonstrating the benefit of flexible intra-chunk alignments for translation tasks.

4.3. Computational Efficiency

Figure 1 compares the GPU memory usage when training RNN-T and CHAT models for one epoch on 5000 selected utterances of Librispeech train, with batch=32. As we can see, CHAT uses around half the memory compared to RNN-T (-46.2% peak memory), and also finish the training 1.36X faster. This is mainly due to RNN-T requiring a tensor of shape [B, T, U, V] as the joiner output, and with CHAT, T is reduced by the factor of the chunk-size (12 in our case). The

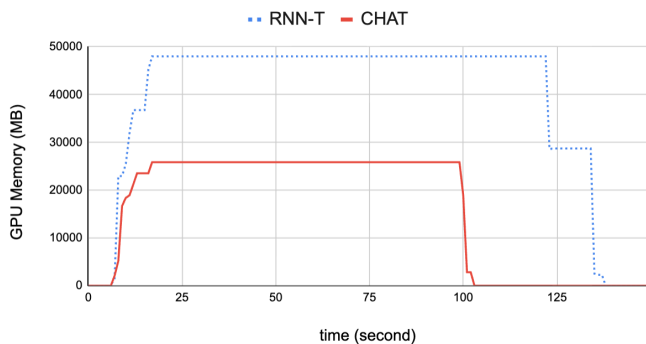


Fig. 1: GPU Memory Usage (MB) when training RNNT and CHAT models for one mini-epoch with batch=32 (5000 selected utterances in Librispeech train) on A6000 GPU.

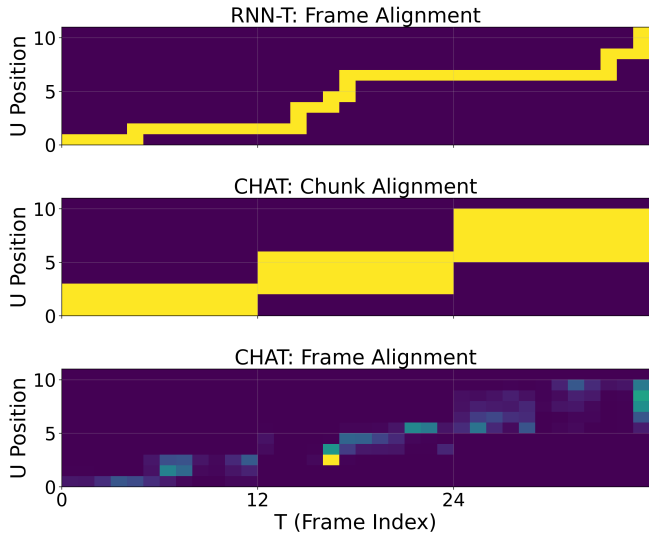


Fig. 2: From top to bottom: 1. RNN-T frame alignments; 2. CHAT chunk-based alignments; 3. CHAT frame-based alignments. Chunk-size = 12.

total memory usage does not scale with $1/\text{chunk-size}$ because the model encoder also takes a lot of memory space.

5. ANALYSIS

5.1. Alignment Visualization

Figure 2 compares attention patterns acquired by running AST inference on the same audio. Besides frame-level alignment of RNN-T and chunk-level alignment of CHAT, we also show frame-level alignment of CHAT, which divides the chunk-based alignment among frames in the chunk, according to attention weights computed at that inference step⁴. We see that the frame-level RNN-T and chunk-level CHAT alignments are strictly monotonic, inside chunks in CHAT models, there can be more intricate patterns where multiple frames are utilized in emission.

5.2. Other Chunk Sizes

In Table 3, we present EN-DE AST results for the RNN-T and CHAT models, trained on more chunk sizes, in addition to the 12 we previously reported. We see that CHAT outperforms RNN-T consistently, regardless of the chunk-size.

5.3. Batched Inference

We also implemented highly optimized label-looping [12] batched inference for CHAT. Table 4 compares the batched

⁴Attention weights are summed across all heads to clearly mark the contribution of frames.

Table 3: En-DE AST BLEU with different chunk-sizes

model	chunk=6	chunk=12	chunk=24	chunk=36
RNN-T	26.63	29.44	29.57	30.60
CHAT	31.16	32.33	33.45	33.63

decoding speed with RNN-T running EN-DE AST on Covost. We see that CHAT runs consistently faster than RNN-T regardless of the batch-size used.

Table 4: Comparison on batched inference speed (total seconds to decode the whole covost testset) with EN-DE AST.

batch	2	4	8	16
RNN-T	288	182	115	84
CHAT	221	125	77	56

5.4. Latency Measurements

Table 5 analyzes the latency characteristics of RNN-T and CHAT models. Ideally, we would measure the true acoustic latency—the delay between when a word is actually spoken and when it’s emitted by the model. However, this requires datasets with precise word-level timing annotations, which are not available for most test sets. Instead, we measure the average timestamp of token emissions relative to utterance start. For chunk-based models, all tokens from a given chunk are emitted at the chunk boundary. This metric serves as a reliable proxy for true acoustic latency, differing only by a constant offset that affects both models equally. The results show nearly identical emission timestamps between RNN-T and CHAT (around 1% difference), indicating that CHAT preserves the temporal characteristics of RNN-T while providing the substantial accuracy and efficiency improvements demonstrated in previous sections.

Table 5: Averaged chunkwise token time-stamp in inference.

model	clean	other
RNN-T	6346ms	5712ms
CHAT	6422ms	5779ms

6. CONCLUSION

We present Chunk-wise Attention Transducer (CHAT), a novel architecture that combines the streaming capabilities of RNN-T with the alignment flexibility of attention-based models. By processing audio in fixed-size chunks and applying attention within chunks, CHAT achieves significant improvements in both accuracy and computational efficiency. Future work will explore adaptive chunk sizing and extension to other sequence-to-sequence tasks.

7. REFERENCES

- [1] Y. He, T. N. Sainath, R. Prabhavalkar *et al.*, “Streaming end-to-end speech recognition for mobile devices,” in *ICASSP*, 2019.
- [2] A. Graves, “Sequence transduction with recurrent neural networks,” *arXiv preprint arXiv:1211.3711*, 2012.
- [3] H. Xu, F. Jia, S. Majumdar, S. Watanabe, and B. Ginsburg, “Multi-blank transducers for speech recognition,” *arXiv:2211.03541*, 2022.
- [4] H. Xu, F. Jia, S. Majumdar, H. Huang, S. Watanabe, and B. Ginsburg, “Efficient sequence transduction by jointly predicting tokens and durations,” in *International Conference on Machine Learning*. PMLR, 2023, pp. 38 462–38 484.
- [5] H. Xu, T. M. Bartley, V. Bataev, and B. Ginsburg, “Hainan: Fast and accurate transducer for hybrid-autoregressive asr,” *arXiv preprint arXiv:2410.02597*, 2024.
- [6] A. Vaswani, N. Shazeer, N. Parmar, J. Uszkoreit, L. Jones, A. N. Gomez, Ł. Kaiser, and I. Polosukhin, “Attention is all you need,” *Advances in neural information processing systems*, vol. 30, 2017.
- [7] A. Gulati, J. Qin, C.-C. Chiu, N. Parmar, Y. Zhang, J. Yu, W. Han, S. Wang, Z. Zhang, Y. Wu *et al.*, “Conformer: Convolution-augmented transformer for speech recognition,” *arXiv preprint arXiv:2005.08100*, 2020.
- [8] M. Ghodsi, X. Liu, J. Apfel, R. Cabrera, and E. Weinstein, “RNN-Transducer with stateless prediction network,” in *ICASSP*, 2020.
- [9] J. Xue, P. Wang, J. Li, M. Post, and Y. Gaur, “Large-scale streaming end-to-end speech translation with neural transducers,” *arXiv preprint arXiv:2204.05352*, 2022.
- [10] H. Xu, V. Bataev, L. Grigoryan, and B. Ginsburg, “Wind: Accelerated rnn-t decoding with windowed inference for non-blank detection,” *arXiv preprint arXiv:2505.13765*, 2025.
- [11] D. Galvez, V. Bataev, H. Xu, and T. Kaldewey, “Speed of light exact greedy decoding for rnn-t speech recognition models on gpu,” *arXiv:2406.03791*, 2024.
- [12] V. Bataev, H. Xu, D. Galvez, V. Lavrukhin, and B. Ginsburg, “Label-looping: Highly efficient decoding for transducers,” *arXiv:2406.06220*, 2024.
- [13] M. Zeineldeen, A. Zeyer, R. Schlüter, and H. Ney, “Chunked attention-based encoder-decoder model for streaming speech recognition,” in *ICASSP 2024-2024 IEEE International Conference on Acoustics, Speech and Signal Processing (ICASSP)*. IEEE, 2024, pp. 11 331–11 335.
- [14] V. Noroozi, S. Majumdar, A. Kumar, J. Balam, and B. Ginsburg, “Stateful conformer with cache-based inference for streaming automatic speech recognition,” in *ICASSP 2024-2024 IEEE International Conference on Acoustics, Speech and Signal Processing (ICASSP)*. IEEE, 2024, pp. 12 041–12 045.
- [15] O. Kuchaiev, J. Li, H. Nguyen *et al.*, “Nemo: a toolkit for building ai applications using neural modules,” in *NeurIPS Workshop on Systems for ML*, 2019.
- [16] D. Rekish, N. R. Koluguri, S. Kriman, S. Majumdar, V. Noroozi *et al.*, “Fast Conformer with linearly scalable attention for efficient speech recognition,” in *Automatic Speech Recognition and Understanding Workshop (ASRU)*, 2023.
- [17] R. Ardila, M. Branson, K. Davis, M. Henretty, M. Kohler, J. Meyer, R. Morais, L. Saunders, F. M. Tyers, and G. Weber, “Common voice: A massively-multilingual speech corpus,” *arXiv:1912.06670*, 2019.
- [18] C. Wang, M. Riviere, A. Lee, A. Wu, C. Talnikar, D. Haziza, M. Williamson, J. Pino, and E. Dupoux, “VoxPopuli: A large-scale multilingual speech corpus for representation learning, semi-supervised learning and interpretation,” in *Proc. of the 59th Annual Meeting of the ACL and the 11th International Joint Conf. on NLP*, 2021.
- [19] V. Pratap, Q. Xu, A. Sriram, G. Synnaeve, and R. Collobert, “MLS: A large-scale multilingual dataset for speech research,” in *Interspeech*, 2020.
- [20] O. Hrinchuk, V. Noroozi, A. Khattar, A. Peganov, S. Subramanian, S. Majumdar, and O. Kuchaiev, “Nvidia nemo offline speech translation systems for iwslt 2022,” in *Proceedings of the 19th International Conference on Spoken Language Translation (IWSLT 2022)*, 2022, pp. 225–231.
- [21] C. Wang, A. Wu, and J. Pino, “Covost 2 and massively multilingual speech-to-text translation,” *arXiv preprint arXiv:2007.10310*, 2020.